

Artificial molecules in coupled and single quantum dots

S. Bednarek, T. Chwiej, J. Adamowski,* and B. Szafran

Faculty of Physics and Nuclear Techniques, University of Mining and Metallurgy (AGH), Kraków, Poland

(Received 16 January 2003; published 21 May 2003)

An exactly solvable model has been proposed for the artificial molecules composed of two electrons confined in double coupled and single isolated quantum dots. This model allows us to study systematically the spontaneous symmetry breaking, which results from the electron-electron correlation in the artificial molecules. By comparing the exact and Hartree-Fock results we have shown that—in the barrier-separated coupled quantum dots—the correlation increases with the increasing barrier thickness, which leads to the localization of both the electrons in the different dots, i.e., the vanishing probability of finding both the electrons in the same dot. In the single quantum dot, the correlation increases with the increasing dot size, which leads to a formation of a Wigner molecule. We have found a remarkable similarity of the electron density distribution in both the types of the artificial molecules.

DOI: 10.1103/PhysRevB.67.205316

PACS number(s): 73.21.-b

I. INTRODUCTION

A quantum dot (QD), i.e., a nanostructure, in which the electrons are confined in all three space dimensions, is called an artificial atom.^{1,2} The electrons confined in the two coupled QD's can form an artificial molecule.³⁻⁸ The artificial-molecule states can be formed in the vertically^{8,9} as well as laterally coupled QD's.¹⁰ The nanostructure with the vertically coupled QD's fabricated by Austing *et al.*⁹ consists of GaAs, AlGaAs, and InGaAs layers, which were etched to form a pillar. Along the axis of the etched pillar (in the vertical direction) the confinement potential can be approximated by the double-well (triple-barrier) potential. The electrons are confined in the QD regions within the two InGaAs layers by this vertical confinement potential and by the lateral confinement potential, which is created by the gate voltage applied to a side gate electrode.

Another class of the artificial molecules can be created in a single isolated QD at high magnetic field.^{11,12} If the magnetic field is sufficiently strong, the electrons can be localized at different sites within the single QD forming a Wigner molecule.¹²

A theory of artificial molecules in single and double QD's deals with few-electron problems, which do not admit exact solutions even for simple parabolic confining potentials. Several approximate methods have been applied to solve the few-electron eigenvalue problem in the QD's. These include the Hartree-Fock (HF),^{13,14} configuration-interaction (CI),^{3,15} and local-density approximation^{6,7,10,16} methods. The CI method with a large number of Slater determinants yields large matrices that can be exactly diagonalized, which allows us to approach the exact solutions.¹⁷ Another possible method to obtain the exact results is based on the real-space mesh techniques^{18,19} that provide accurate numerical solutions. However, the singularity of the Coulomb potential at small interparticle distances limits the accuracy of the techniques based on the finite differences.¹⁸ The Coulomb singularity is especially hard to overcome in problems with the reduced dimensionality, e.g., one-dimensional (1D) problems, which arise when considering the electrons confined in the 1D QD's (Ref. 11) and quantum wires.²⁰ Moreover, when

applying the path-integral method to the QD's,²¹ one obtains systematic overestimates of the energy of the system with the Coulomb interaction. Therefore, it is desirable to replace the Coulomb interaction by some nonsingular effective interaction, which could simulate the behavior of the confined-electron system and lead to exact solutions (at least for the small number of electrons).

In the present paper, we propose such an effective inter-electron interaction, which allows us to reduce the original three-dimensional (3D) electron problem to the effective, exactly solvable, 1D problem. Using this effective interaction we obtain the exact solutions for the two-electron artificial molecules in the single isolated QD and double coupled QD's. For the single QD, we study the conditions, under which the electrons form the Wigner molecule and discuss the similarity between the artificial molecules created in the single and double QD's. The paper is organized as follows: Section II contains the description of the theoretical model with the derivation of the effective interaction, Sec. III contains the results, and Sec. IV, the discussion and conclusions.

II. THEORETICAL MODEL

We consider the cylindrically symmetric 3D electron system confined in the single isolated QD. We assume the confinement potential to be a sum of lateral parabolic (U_{\perp}) and vertical (U_{\parallel}) confinement potentials, i.e.,

$$U_{conf}(\mathbf{r}) = U_{\perp}(x, y) + U_{\parallel}(z). \quad (1)$$

For this separable potential the one-electron wave function is a product

$$\psi(\mathbf{r}) = \psi_{\perp}(x, y) \psi_{\parallel}(z). \quad (2)$$

The lateral potential is assumed to be parabolic, i.e.,

$$U_{\perp}(x, y) = \frac{m\omega_{\perp}^2}{2}(x^2 + y^2), \quad (3)$$

where m is the effective electron band mass and ω_{\perp} is the lateral confinement frequency. The ground state wave function for the lateral motion has the form

$$\psi_{\perp}(x, y) = (2\beta/\pi)^{1/2} \exp[-\beta(x^2 + y^2)], \quad (4)$$

where $\beta = m\omega_{\perp}/2\hbar$.

Let us consider the electron-electron interaction energy

$$U_{12} = \frac{e^2}{4\pi\epsilon_0\epsilon} \int d^3r_1 d^3r_2 \frac{|\Psi(\mathbf{r}_1, \mathbf{r}_2)|^2}{|\mathbf{r}_1 - \mathbf{r}_2|}, \quad (5)$$

where $\Psi(\mathbf{r}_1, \mathbf{r}_2)$ is the two-electron wave function and ϵ is the static dielectric constant. For the parabolic lateral potential and under assumption that the vertical confinement is considerably weaker than the lateral one, we can separate the ground-state two-electron wave function as follows:

$$\Psi(\mathbf{r}_1, \mathbf{r}_2) = \psi_{\perp}(x_1, y_1) \psi_{\perp}(x_2, y_2) \Psi_{\parallel}(z_1, z_2). \quad (6)$$

Substituting this form into Eq. (5) and integrating over the lateral coordinates, we obtain

$$U_{12} = \int_{-\infty}^{\infty} dz_1 \int_{-\infty}^{\infty} dz_2 |\Psi_{\parallel}(z_1, z_2)|^2 U_{eff}(|z_1 - z_2|). \quad (7)$$

In Eq. (7), U_{eff} is the effective 1D electron-electron interaction given by

$$U_{eff}(|z|) = \frac{e^2(\pi\beta)^{1/2}}{4\pi\epsilon_0\epsilon} \operatorname{erfcx}(\beta^{1/2}|z|), \quad (8)$$

where

$$\operatorname{erfcx}(\zeta) = \exp(\zeta^2) \operatorname{erfc}(\zeta) \quad (9)$$

is the exponentially scaled complementary error function.²² The effective interaction energy (8) is essentially Coulombic at large interelectron distances but—contrary to the Coulomb potential—does not possess any singularity at zero distance (Fig. 1). At small distances, the effective interaction is much softer than the Coulomb interaction and possesses a cusp, which stems from the averaged Coulomb singularity at origin. The nonsingular effective interaction (8) can be used to obtain exact solutions for the few-electron problems in the QD's.

The assumption of the separated form of wave function (6), under which Eq. (8) has been obtained, means that the energy-level differences for the quantized motion in the z direction are much smaller than the corresponding differences for the lateral motion. In this case, several low-energy levels of the quantized vertical motion correspond to the ground state of the lateral motion. This assumption is well fulfilled in the QD formed from a section of a quantum wire,²⁰ for which the vertical extension of the QD is much greater than the lateral one. The vertically coupled double QD's⁹ with the same (or comparable) size provide another possible physical realization of the model system considered. In the nanostructure made of the two QD's with the comparable size, the main contribution to the two-electron wave function stems from the single-QD one-electron wave functions, which are associated with comparable energies. Then, the corresponding energy differences for the vertical motion are much smaller than those for the lateral motion and the excited states of the lateral motion only slightly affect the two-electron ground state.

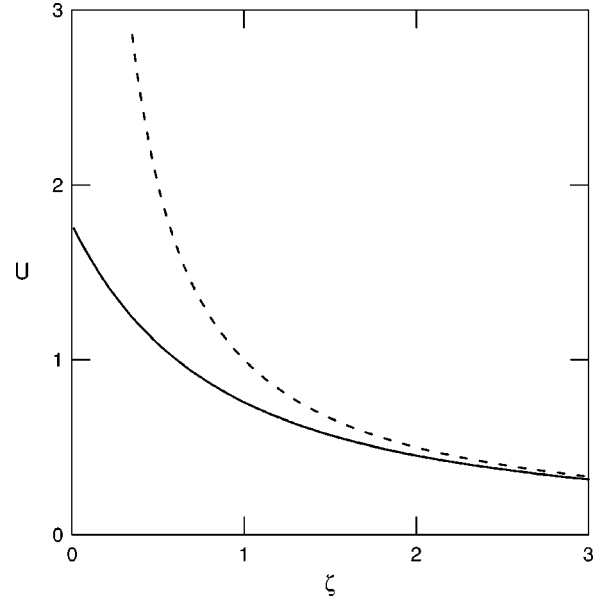


FIG. 1. Effective (solid curve) and Coulomb (dashed curve) electron-electron interaction potentials as functions of electron-electron distance ζ . Length is expressed in units $l_{\perp} = (2\hbar/m\omega_{\perp})^{1/2}$, energy in units $\hbar\omega_{\perp}$, and we take on $R_D = \hbar\omega_{\perp}$, where R_D is the donor rydberg.

The effective electron-electron interaction (8) allows us to simplify considerably the two-electron problem, which—in a general case—depends on the six coordinates. After separating the lateral and vertical motions and using Eq. (8), we can reduce the number of independent coordinates to two. The corresponding two-electron Hamiltonian has the form

$$H(z_1, z_2) = -\frac{\hbar^2}{2m} \left(\frac{\partial^2}{\partial z_1^2} + \frac{\partial^2}{\partial z_2^2} \right) + U_{\parallel}(z_1) + U_{\parallel}(z_2) + U_{eff}(|z_1 - z_2|) + 2\hbar\omega_{\perp}, \quad (10)$$

where the last term is the ground-state energy of the two noninteracting electrons in the two-dimensional (2D) lateral parabolic confinement potential. The two-electron eigenvalue problem with the Hamiltonian (10) is a unique two-electron problem, which can be solved exactly, i.e., with the correlation effects entirely taken into account. This solution has been obtained by the iterative extraction-orthogonalization method,²³ which allows us to achieve an arbitrary precision²⁴ for the eigenvalues and wave functions. In the present paper, we require that the uncertainty of the calculated energy levels does not exceed 10^{-6} meV. Therefore, we can regard these solutions to be exact in the framework of the present model which is based on the assumption of parabolic lateral confinement (3) and separability of wave function (6).

In the present approach, the one-electron approximations are not necessary. Instead, we can study the quality of the approximate methods based on the application of the one-electron wave functions, e.g., HF method, by comparing the exact and approximate solutions. The exact solutions of the two-electron problem—in contrast to the HF solutions—fully take into account the electron-electron correlation. In

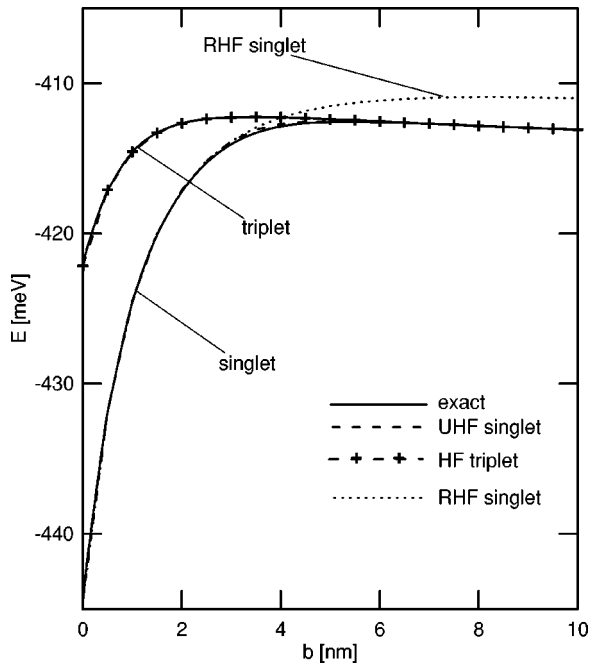


FIG. 2. Lowest singlet (lower solid curve) and triplet (upper solid curve) energy levels of the two-electron system confined in the double QD as functions of barrier thickness b . The UHF (RHF) results for the singlet state are drawn by the dashed (dotted) curve. For the triplet state the results of both the HF methods are the same and are shown by the dashed curve with crosses.

the present paper, we have performed the calculations applying the two versions of the HF method, namely, the restricted HF (RHF) and the unrestricted HF (UHF) method. In the UHF method for all the states and in the RHF method for the triplet states, each one-electron orbital is independently optimized for each spin state. When calculating the singlet states by the RHF method, the one-electron orbitals are the same for the different spin states.

III. RESULTS

A. Coupled quantum dots

The calculations have been performed for the double-barrier vertical confinement potential with the 12-nm well width and depth -240 meV (the energy is measured with respect to the conduction-band minimum of the barrier material). Moreover, we take on $m = 0.064m_e$ for $\text{In}_{0.05}\text{Ga}_{0.95}\text{As}$, $\varepsilon = 12.9$, and $\hbar\omega_{\perp} = 6$ meV. The material parameters used in the calculations correspond to the vertically coupled QD's of Austing *et al.*⁹

We study the artificial-molecule states, which are formed in the two vertically coupled QD's separated by the potential barrier with thickness b . By varying b we can change the coupling between the QD's. Figure 2 shows the exact, UHF, and RHF results for the lowest-energy singlet and triplet states. For the strongly coupled QD's, i.e., for $b \leq 6$ nm, the singlet and triplet states are nondegenerate and the singlet state is the ground state of the system. For $b > 6$ nm, i.e., in the weak coupling regime, the singlet and triplet energy levels become degenerate. We note that the exact results are

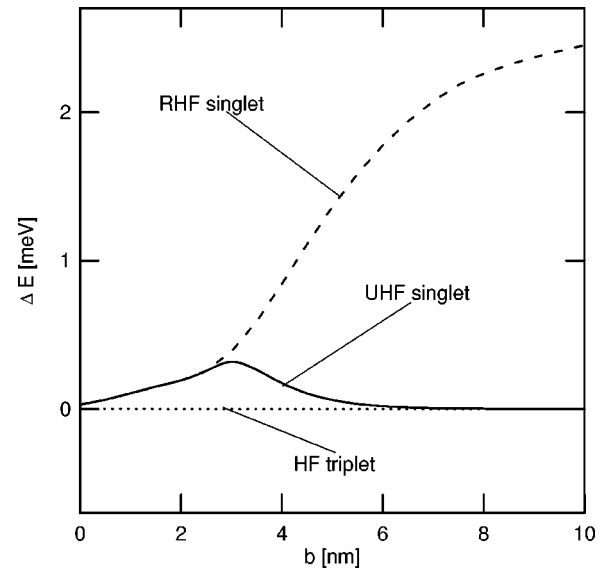


FIG. 3. Estimated error ΔE of the UHF (solid curve) and RHF (dashed curve) methods for the singlet state of two electrons confined in the double QD with barrier thickness b . The errors for the triplet state of both the HF methods are shown by the dotted line.

fairly well reproduced by the UHF method, while the RHF approach considerably overestimates the energy of the singlet state. For $b > 4$ nm the RHF method yields the incorrect ordering of the energy levels (the singlet energy level is erroneously predicted to lie above the triplet level). The results for the triplet state obtained by both the HF methods are the same and are almost indistinguishable from the exact results.

We have studied the accuracy of the HF methods by estimating the errors $\Delta E = |E_{\text{exact}} - E_{\text{HF}}|$, where E_{HF} is the HF energy estimate obtained by either the RHF or UHF method. Usually, the correlation energy is defined as $E_{\text{corr}} = -\Delta E$ with E_{HF} calculated by the RHF method. For the triplet state both the UHF and RHF methods are equivalent and lead to the identical results marked by HF in Figs. 2 and 3. In this state, the HF energy estimates are nearly exact, i.e., the correlation error is negligibly small at all interdot distances. The inaccuracies of the HF methods appear for the singlet state. The error of the UHF method increases with b for small b , is maximal for $b = 3$ nm, and decreases for larger b . For $b > 6$ nm the UHF results become indistinguishable from the exact ones. On the contrary, the RHF energy estimates are remarkably distinct from the exact results at all b and the RHF error monotonically increases with b .

In order to get a more deep physical insight into the properties of the system considered, we have plotted in Fig. 4 the contours of the two-electron probability density, i.e., $|\Psi_{\parallel}(z_1, z_2)|^2$, for the singlet [Fig. 4(a)] and triplet [Fig. 4(b)] states. The case $b = 0$ corresponds to the single QD, in which the two joined potential wells form the single potential well with the double width. For the singlet state and $b = 0$ the electrons are localized nearly at the center of the single QD [cf. Fig. 4(a)]. Nevertheless, the interelectron repulsion slightly shifts the electrons in the opposite directions, which is visible as a small deformation of the exact two-electron wave function. This is a trace of the weak electron-electron

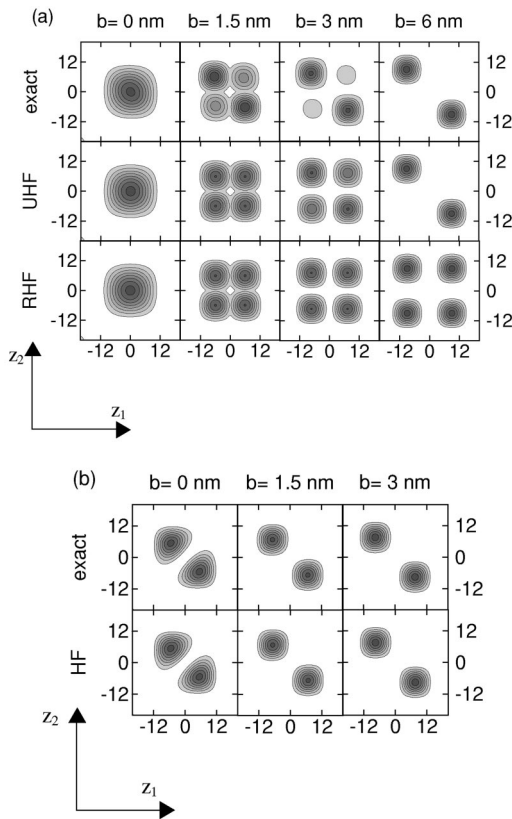


FIG. 4. Contours of the two-electron probability density in the coupled QD's as functions of z_1 and z_2 (in nm) for the singlet (a) and triplet (b) states for several values of barrier thickness b . The darker the shade of gray, the larger the electron density. The white areas correspond to the electron probability density equal to zero.

correlation. If we introduce the barrier with the increasing thickness, the correlation increases and the electrons can be found with the increasing probability in the different QD's. For $b=6$ nm the probability of finding both the electrons in the same QD vanishes. In this case, the correlation is strong. These properties of the exact two-electron wave function are reproduced by the UHF method. However, the redistribution of the electrons over the different QD's occurs with some "delay" when the barrier thickness increases. This leads to the increase of the UHF error for small b and its disappearance for large b . For $b=6$ nm the UHF and exact electron densities are indistinguishable. The ground-state wave function [cf. exact and UHF results in Fig. 4(a)] does not possess the symmetry of the confining potential, i.e., the one-electron parity is not conserved. Only the total parity, which corresponds to the simultaneous inversion of the coordinates of both particles, is well defined for the artificial molecules considered. However, the RHF wave functions are additionally symmetric with respect to the one-electron parity, which leads to the erroneous prediction of equal probabilities of finding one or two electrons in the same QD. In the triplet state, the correlation is negligibly small and the exact and HF wave functions are identical [Fig. 4(b)].

B. Wigner molecules in a single quantum dot

In the double QD, the localization of electrons changes if we change the repulsive potential of the barrier. As a result,

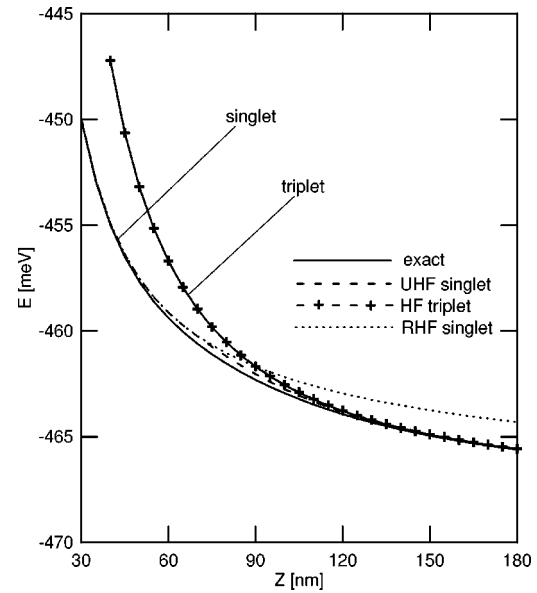


FIG. 5. Lowest singlet (lower solid curve) and triplet (upper solid curve) energy levels of the two-electron system confined in the single QD as functions of linear size Z of the QD. The UHF (RHF) results for the singlet state are drawn by dashed (dotted) curve. For the triplet state the results of both the HF methods are the same and are shown by the dashed curve with crosses.

for the potential barrier with the sufficiently large height and thickness the electrons become spatially separated and localized in the different QD's. The correlation is of crucial importance in the separation of the electrons between the different dots. In the single isolated QD, the electron-electron correlation can also be responsible for the localization of the electrons. In order to show this effect we have performed the calculations for the two-electron system in the single QD with the varying size and with the same values of the other parameters as those for the double QD. Figure 5 shows that—similarly as for the double QD—the singlet state is the ground state of the system and the singlet and triplet states become degenerate if the size of the QD exceeds ~ 120 nm. Like in the double QD, the results for the singlet state are fairly well reproduced by the UHF method, while the RHF approach leads to a considerable overestimation of the ground-state energy, which increases with the increasing size of the QD. Moreover, the RHF method erroneously predicts the triplet state to be the ground state for the QD's of a large size. The corresponding errors are displayed in Fig. 6. Similarly as in the coupled QD's, the error of the UHF method for the singlet state grows with the size of the QD, reaches the maximum at $Z=75$ nm, and next decreases to zero. The RHF error is a monotonically increasing function of the QD size. In the triplet state, the HF error is negligibly small.

Let us look at the electron density distribution in the single QD (Fig. 7). If the size of the dot increases, the electrons in the singlet state tend to be localized at the different sites of the QD [cf. exact results in Fig. 7(a) for $Z \geq 70$ nm]. The results for $Z=70$ and 100 nm can be interpreted as a creation of precursors of Wigner molecules.^{11,12} If Z is larger than ~ 120 nm, the electrons become strongly

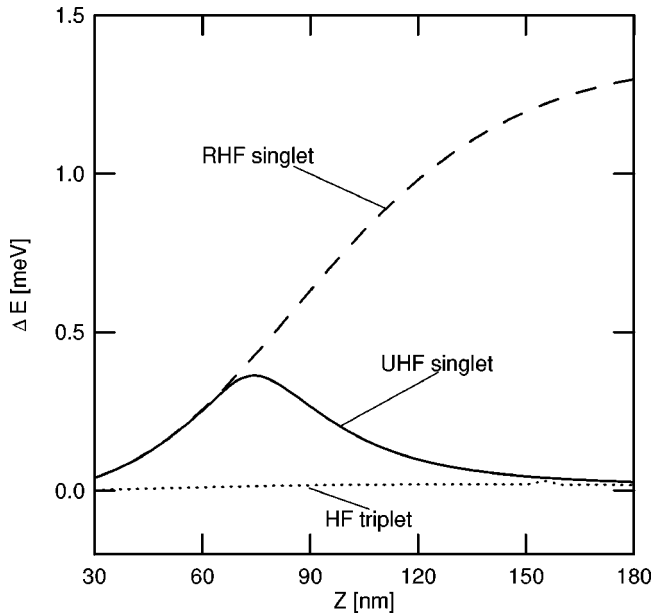


FIG. 6. Estimated error ΔE of the UHF (solid curve) and RHF (dashed curve) methods for the singlet state of two electrons confined in the single QD as a function of linear size Z of the QD. For the triplet state the errors of both the HF methods are shown by the dotted line.

localized at the different sites within the QD. In this case, the Wigner molecule^{11,12} is formed with the clearly separated electrons. The Wigner molecules can be created in the singlet [Fig. 7(a)] as well as in the triplet [Fig. 7(b)] state. It is interesting that—contrary to the magnetic-field induced formation of the Wigner molecules¹²—no external field is necessary to create the Wigner molecules of this kind. In the present case, the formation of the Wigner molecules results from the strong electron-electron correlation. This effect is well reproduced by the UHF method (cf. Figs. 5 and 6), but not by the RHF method. Comparing Fig. 4(a) with Fig. 7(a) and Fig. 4(b) with Fig. 7(b) we note the remarkable similarity of the electron density distributions in the artificial molecules formed in the double and single QD's.

IV. DISCUSSION AND CONCLUSIONS

We have considered the 3D problem of interacting electrons in double and single QD's. The assumption of the harmonic-oscillator potential for the lateral confinement (3) and the separability of wave function (6) allows us to reduce the 3D problem to the 1D problem. The effective electron-electron interaction obtained is a smooth nonsingular function of the interelectron distance with the long-range Coulomb tail. These properties of the effective interaction enable us to solve the two-electron problem exactly. In the present paper, the effective interaction has been applied to the two-electron artificial molecules created in the double and single QD's.

In quantum wells, the effective electron-electron interaction has been studied by Price *et al.*²⁵ The authors²⁵ performed the averaging over the electron ground state in the vertical direction and obtained the effective interaction in the

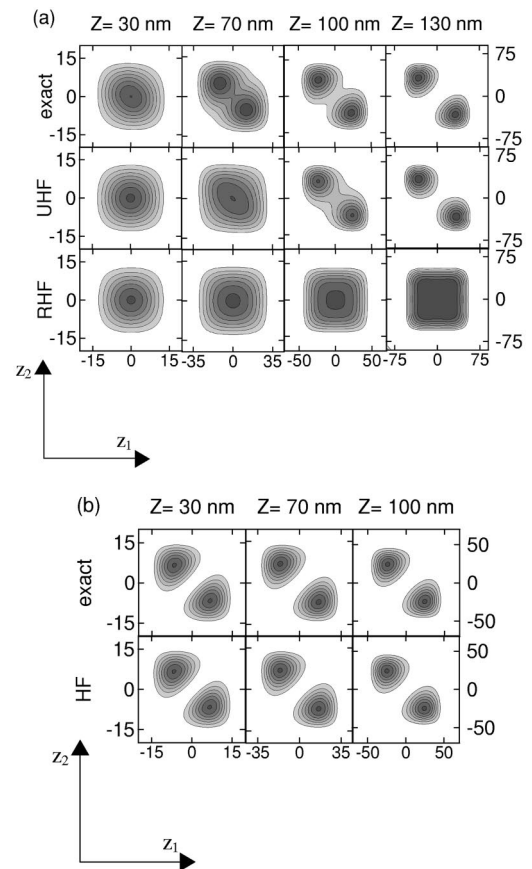


FIG. 7. Contours of the two-electron electron probability density in the single QD as functions of z_1 and z_2 (in nm) for the singlet (a) and triplet (b) states for several values of dot size Z . Note the different length scales for different Z . The gray scale is as in Fig. 4.

lateral direction, which is qualitatively similar to U_{eff} [Eq. (8)]. However, in the calculations, the authors²⁵ preferred to use the simpler model interaction, which at small distances—on the contrary to Eq. (8)—possesses the flat, parabolic-like maximum. The parabolic form is also characteristic for the model interaction proposed by Johnson and Payne.²⁶ According to the derivation presented in Sec. II and that given by Price *et al.*,²⁵ the effective interaction should have a cusp at zero interelectron distance (cf. Fig. 1), which results from the Coulomb singularity at origin.

The problem of two electrons in the quasi-1D coupled QD's was considered by Tamborenea and Metiu,²⁰ who, however, did not derive a closed formula for the effective interaction. Jauregui *et al.*¹¹ investigated the formation of Wigner molecules in quasi-1D QD's using the model interaction.²⁵ Yannouleas and Landman⁵ discussed the spontaneous symmetry breaking in the single and laterally coupled QD's applying the two-center-oscillator confinement. The results for the planar two-dot system⁵ exhibit a qualitative similarity to the present results for the vertically coupled QD's.

The effective electron-electron interaction proposed in the present paper can be used together with the model confinement potential, which is sufficiently flexible to account for the realistic confinement. In Ref. 27, we have proposed the

power-exponential confinement potential, which allows us to model the properties of real QD's.

In order to study the correlation effects we have performed calculations with the use of both the RHF and UHF methods. We have found that the UHF method fairly accurately takes into account the electron-electron correlation. The deviations of the UHF results from the exact ones occur only for the small barrier thickness in the double QD and for the small size of the single QD. If the barrier thickness in the coupled QD's (linear size of the single QD) increases, the UHF results become indistinguishable from the exact ones. In particular, both the exact and UHF methods predict the formation of the Wigner molecule in the single QD with the sufficiently large size. When the Wigner molecule is created, the Coulomb interaction potential energy dominates over the other energy contributions. In this case, the confining-potential symmetry of the two-electron wave function is broken, which leads to the localization of the electrons at the different sites of the QD. Due to the application of the same electron orbitals for the singlet states, the RHF method does not allow for this symmetry breaking and does not lead to the formation of the Wigner molecule.

It is interesting that the spontaneous breaking of the symmetry of the confining potential leads to the very similar electron density distributions in the different types of the artificial molecules studied, namely, the artificial molecules formed in the double coupled QD's and the Wigner molecules formed in the single isolated QD. In both the cases, the redistribution and localization of the electrons results from the electron-electron correlation, which becomes strong for the nanostructures of the sufficiently large size.

In the coupled QD's, the electron-electron correlation in-

creases with the increasing thickness of the barrier layer separating the dots. This means that—in some sense—the correlation can be artificially tuned by changing the thickness of the barrier layer. Therefore, in the double coupled QD nanostructure, we can intentionally change the electron-electron correlation from weak (for the thin barrier) to strong (for the thick barrier). The same tuning of the correlation can be realized in the single QD by changing its size.

In summary, we have proposed the model for the 3D electron systems confined in single and double QD's, which allows us to obtain numerical solutions of the arbitrary required precision within the present model for the two-electron artificial molecules. The effective interaction obtained in the present paper can also be applied to the many-electron systems. We have determined the conditions under which the electrons are strongly localized in the different QD's in the double-dot structure and in the spatially separated parts of the single QD. We have obtained accurate results that allow us to study systematically the formation and evolution of Wigner molecules from the weakly to strongly correlated systems. We have found that the electron density distribution in both types of the artificial molecules studied show a remarkable similarity. Additionally, we have discussed the accuracy of the HF methods and pointed out that the UHF method leads to the exact results for the two-electron Wigner molecules and for the two-electron systems confined in the weakly coupled QD's.

ACKNOWLEDGMENT

This work has been partly supported by the Polish Government Scientific Research Committee (KBN) under Grant No. 5P03B 4920.

*Email address: adamowski@ftj.agh.edu.pl

¹P. A. Maksym and T. Chakraborty, Phys. Rev. Lett. **65**, 108 (1990).

²M. A. Kastner, Phys. Today **46**(1), 24 (1993).

³G. W. Bryant, Phys. Rev. B **48**, 8024 (1993).

⁴J. J. Palacios and P. Hawrylak, Phys. Rev. B **51**, 1769 (1995).

⁵C. Yannouleas and U. Landman, Phys. Rev. Lett. **82**, 5325 (1999).

⁶B. Partoens and F. M. Peeters, Phys. Rev. Lett. **84**, 4433 (2000).

⁷M. Pi, A. Emperador, M. Barranco, and F. Garcias, Phys. Rev. B **63**, 115316 (2001).

⁸M. Pi, A. Emperador, M. Barranco, F. Garcias, K. Muraki, S. Tarucha, and D. G. Austing, Phys. Rev. Lett. **87**, 066801 (2001).

⁹D. G. Austing, T. Honda, K. Muraki, Y. Tokura, and S. Tarucha, Physica B **249–251**, 206 (1998).

¹⁰S. Nagaraja, J.-P. Leburton, and R. M. Martin, Phys. Rev. B **60**, 8759 (1999).

¹¹K. Jauregui, W. Häusler, and B. Kramer, Europhys. Lett. **24**, 581 (1993).

¹²B. Szafran, S. Bednarek, and J. Adamowski, Phys. Rev. B **67**, 045311 (2003).

¹³H.-M. Müller and S. E. Koonin, Phys. Rev. B **54**, 14 532 (1996).

¹⁴S. Bednarek, B. Szafran, and J. Adamowski, Phys. Rev. B **64**, 195303 (2001).

¹⁵M. Eto, J. Appl. Phys. **36**, 3924 (1997).

¹⁶O. Steffens, U. Rössler, and M. Suhrke, Europhys. Lett. **42**, 529 (1998).

¹⁷A. Wojs and P. Hawrylak, Phys. Rev. B **53**, 10 841 (1996).

¹⁸J. R. Chelikowsky, N. Troullier, K. Wu, and Y. Saad, Phys. Rev. B **50**, 11 355 (1994).

¹⁹T. L. Beck, Rev. Mod. Phys. **72**, 1041 (2000).

²⁰P. I. Tamborenea and H. Metiu, Phys. Rev. Lett. **83**, 3912 (1999).

²¹E. P. Pokatilov, V. M. Fomin, J. T. Devreese, S. N. Balaban, and S. N. Klimin, Phys. Rev. B **61**, 2721 (2000).

²²Y. L. Luke, *The Special Functions and Their Approximations*, Vol. 1 (Academic, New York, 1969).

²³R. Kosloff and H. Tal-Ezer, Chem. Phys. Lett. **127**, 223 (1986); D. Jovanovic and J.-P. Leburton, Phys. Rev. B **49**, 7474 (1994).

²⁴B. Szafran, J. Adamowski, and S. Bednarek, Physica E (Amsterdam) **5**, 185 (2000).

²⁵R. Price, X. Zhu, S. Das Sarma, and P. M. Platzman, Phys. Rev. B **51**, 2017 (1995).

²⁶N. F. Johnson and M. C. Payne, Phys. Rev. B **45**, 3819 (1992).

²⁷M. Ciurla, J. Adamowski, B. Szafran, and S. Bednarek, Physica E (Amsterdam) **15**, 261 (2002).